

12-29-2011

Measurement of the B_s^0 lifetime in fully and partially reconstructed $B_s^0 \rightarrow D_s^-(\Phi\pi^+)X$ decays in $\bar{p}p$ collisions at $\sqrt{s}=1.96\text{TeV}$

T. Aaltonen
Helsingin Yliopisto

B. Álvarez González
Universidad de Cantabria

S. Amerio
Istituto Nazionale Di Fisica Nucleare, Sezione di Padova

D. Amidei
University of Michigan, Ann Arbor

A. Anastassov
Northwestern University

See next page for additional authors https://digitalcommons.lsu.edu/physics_astronomy_pubs

Recommended Citation

Aaltonen, T., Álvarez González, B., Amerio, S., Amidei, D., Anastassov, A., Annovi, A., Antos, J., Apollinari, G., Appel, J., Apresyan, A., Arisawa, T., Artikov, A., Asaadi, J., Ashmanskas, W., Auerbach, B., Aurisano, A., Azfar, F., Badgett, W., Barbaro-Galtieri, A., Barnes, V., Barnett, B., Barria, P., Bartos, P., Bauce, M., Bauer, G., Bedeschi, F., Beecher, D., & Behari, S. (2011). Measurement of the B_s^0 lifetime in fully and partially reconstructed $B_s^0 \rightarrow D_s^-(\Phi\pi^+)X$ decays in $\bar{p}p$ collisions at $\sqrt{s}=1.96\text{TeV}$. *Physical Review Letters*, 107 (27) <https://doi.org/10.1103/PhysRevLett.107.272001>

This Article is brought to you for free and open access by the Department of Physics & Astronomy at LSU Digital Commons. It has been accepted for inclusion in Faculty Publications by an authorized administrator of LSU Digital Commons. For more information, please contact ir@lsu.edu.

Authors

T. Aaltonen, B. Álvarez González, S. Amerio, D. Amidei, A. Anastassov, A. Annovi, J. Antos, G. Apollinari, J. A. Appel, A. Apresyan, T. Arisawa, A. Artikov, J. Asaadi, W. Ashmanskas, B. Auerbach, A. Aurisano, F. Azfar, W. Badgett, A. Barbaro-Galtieri, V. E. Barnes, B. A. Barnett, P. Barria, P. Bartos, M. Bauce, G. Bauer, F. Bedeschi, D. Beecher, and S. Behari



CHORUS

This is the accepted manuscript made available via CHORUS. The article has been published as:

Measurement of the $B_{\{s\}}^{\{0\}}$ Lifetime in Fully and Partially Reconstructed $B_{\{s\}}^{\{0\}} \rightarrow D_{\{s\}}^{\{-\}} (\phi \pi^{\{-\}}) X$ Decays in $p[\overline{}]p$ Collisions at $\sqrt{s}=1.96$ TeV

T. Aaltonen *et al.* (CDF Collaboration)

Phys. Rev. Lett. **107**, 272001 — Published 29 December 2011

DOI: [10.1103/PhysRevLett.107.272001](https://doi.org/10.1103/PhysRevLett.107.272001)

**Measurement of the B_s^0 Lifetime in Fully and Partially Reconstructed
 $B_s^0 \rightarrow D_s^-(\phi\pi^-)X$ Decays in $\bar{p}p$ Collisions at $\sqrt{s} = 1.96$ TeV**

T. Aaltonen,²¹ B. Álvarez González^{v,9} S. Amerio,⁴¹ D. Amidei,³² A. Anastassov,³⁶ A. Annovi,¹⁷ J. Antos,¹² G. Apollinari,¹⁵ J.A. Appel,¹⁵ A. Apresyan,⁴⁶ T. Arisawa,⁵⁶ A. Artikov,¹³ J. Asaadi,⁵¹ W. Ashmanskas,¹⁵ B. Auerbach,⁵⁹ A. Aurisano,⁵¹ F. Azfar,⁴⁰ W. Badgett,¹⁵ A. Barbaro-Galtieri,²⁶ V.E. Barnes,⁴⁶ B.A. Barnett,²³ P. Barria^{cc,44} P. Bartos,¹² M. Bauce^{aa,41} G. Bauer,³⁰ F. Bedeschi,⁴⁴ D. Beecher,²⁸ S. Behari,²³ G. Bellettini^{bb,44} J. Bellinger,⁵⁸ D. Benjamin,¹⁴ A. Beretvas,¹⁵ A. Bhatti,⁴⁸ M. Binkley^{*,15} D. Bisello^{aa,41} I. Bizjak^{gg,28} K.R. Bland,⁵ B. Blumenfeld,²³ A. Bocci,¹⁴ A. Bodek,⁴⁷ D. Bortoletto,⁴⁶ J. Boudreau,⁴⁵ A. Boveia,¹¹ B. Brau^{a,15} L. Brigliadori^{z,6} A. Brisuda,¹² C. Bromberg,³³ E. Brucken,²¹ M. Bucchiantonio^{bb,44} J. Budagov,¹³ H.S. Budd,⁴⁷ S. Budd,²² K. Burkett,¹⁵ G. Busetto^{aa,41} P. Bussey,¹⁹ A. Buzatu,³¹ C. Calancha,²⁹ S. Camarda,⁴ M. Campanelli,³³ M. Campbell,³² F. Canelli^{12,15} A. Canepa,⁴³ B. Carls,²² D. Carlsmith,⁵⁸ R. Carosi,⁴⁴ S. Carrillo^{k,16} S. Carron,¹⁵ B. Casal,⁹ M. Casarsa,¹⁵ A. Castro^{z,6} P. Catastini,¹⁵ D. Cauz,⁵² V. Cavaliere^{cc,44} M. Cavalli-Sforza,⁴ A. Cerri^{f,26} L. Cerrito^{q,28} Y.C. Chen,¹ M. Chertok,⁷ G. Chiarelli,⁴⁴ G. Chlachidze,¹⁵ F. Chlebana,¹⁵ K. Cho,²⁵ D. Chokheli,¹³ J.P. Chou,²⁰ W.H. Chung,⁵⁸ Y.S. Chung,⁴⁷ C.I. Ciobanu,⁴² M.A. Ciocci^{cc,44} A. Clark,¹⁸ G. Compostella^{aa,41} M.E. Convery,¹⁵ J. Conway,⁷ M. Corbo,⁴² M. Cordelli,¹⁷ C.A. Cox,⁷ D.J. Cox,⁷ F. Crescioli^{bb,44} C. Cuenca Almenar,⁵⁹ J. Cuevas^{v,9} R. Culbertson,¹⁵ D. Dagenhart,¹⁵ N. d'Ascenzo^{t,42} M. Datta,¹⁵ P. de Barbaro,⁴⁷ S. De Cecco,⁴⁹ A. Deisher,^{8,26} G. De Lorenzo,⁴ M. Dell'Orso^{bb,44} C. Deluca,⁴ L. Demortier,⁴⁸ J. Deng^{c,14} M. Deninno,⁶ F. Devoto,²¹ M. d'Errico^{aa,41} A. Di Canto^{bb,44} B. Di Ruzza,⁴⁴ J.R. Dittmann,⁵ M. D'Onofrio,²⁷ S. Donati^{bb,44} P. Dong,¹⁵ T. Dorigo,⁴¹ K. Ebina,⁵⁶ A. Elagin,⁵¹ A. Eppig,³² R. Erbacher,⁷ D. Errede,²² S. Errede,²² N. Ershaidat^{y,42} R. Eusebi,⁵¹ H.C. Fang,²⁶ S. Farrington,⁴⁰ M. Feindt,²⁴ J.P. Fernandez,²⁹ C. Ferrazza^{dd,44} R. Field,¹⁶ G. Flanagan^{r,46} R. Forrest,⁷ M.J. Frank,⁵ M. Franklin,²⁰ J.C. Freeman,¹⁵ I. Furic,¹⁶ M. Gallinaro,⁴⁸ J. Galyardt,¹⁰ J.E. Garcia,¹⁸ A.F. Garfinkel,⁴⁶ P. Garosi^{cc,44} H. Gerberich,²² E. Gerchtein,¹⁵ S. Giagu^{ee,49} V. Giakoumopoulou,³ P. Giannetti,⁴⁴ K. Gibson,⁴⁵ C.M. Ginsburg,¹⁵ N. Giokaris,³ P. Giromini,¹⁷ M. Giunta,⁴⁴ G. Giurgiu,²³ V. Glagolev,¹³ D. Glenzinski,¹⁵ M. Gold,³⁵ D. Goldin,⁵¹ N. Goldschmidt,¹⁶ A. Golossanov,¹⁵ G. Gomez,⁹ G. Gomez-Ceballos,³⁰ M. Goncharov,³⁰ O. González,²⁹ I. Gorelov,³⁵ A.T. Goshaw,¹⁴ K. Goulianos,⁴⁸ A. Gresele,⁴¹ S. Grinstein,⁴ C. Grosso-Pilcher,¹¹ R.C. Group,⁵⁵ J. Guimaraes da Costa,²⁰ Z. Gunay-Unalan,³³ C. Haber,²⁶ S.R. Hahn,¹⁵ E. Halkiadakis,⁵⁰ A. Hamaguchi,³⁹ J.Y. Han,⁴⁷ F. Happacher,¹⁷ K. Hara,⁵³ D. Hare,⁵⁰ M. Hare,⁵⁴ R.F. Harr,⁵⁷ K. Hatakeyama,⁵ C. Hays,⁴⁰ M. Heck,²⁴ J. Heinrich,⁴³ M. Herndon,⁵⁸ S. Hewamanage,⁵ D. Hidas,⁵⁰ A. Hocker,¹⁵ W. Hopkins^{g,15} D. Horn,²⁴ S. Hou,¹ R.E. Hughes,³⁷ M. Hurwitz,¹¹ U. Husemann,⁵⁹ N. Hussain,³¹ M. Hussein,³³ J. Huston,³³ G. Introzzi,⁴⁴ M. Iori^{ee,49} A. Ivanov^{o,7} E. James,¹⁵ D. Jang,¹⁰ B. Jayatilaka,¹⁴ E.J. Jeon,²⁵ M.K. Jha,⁶ S. Jindariani,¹⁵ W. Johnson,⁷ M. Jones,⁴⁶ K.K. Joo,²⁵ S.Y. Jun,¹⁰ T.R. Junk,¹⁵ T. Kamon,⁵¹ P.E. Karchin,⁵⁷ Y. Kato^{n,39} W. Ketchum,¹¹ J. Keung,⁴³ V. Khotilovich,⁵¹ B. Kilminster,¹⁵ D.H. Kim,²⁵ H.S. Kim,²⁵ H.W. Kim,²⁵ J.E. Kim,²⁵ M.J. Kim,¹⁷ S.B. Kim,²⁵ S.H. Kim,⁵³ Y.K. Kim,¹¹ N. Kimura,⁵⁶ M. Kirby,¹⁵ S. Klimenko,¹⁶ K. Kondo,⁵⁶ D.J. Kong,²⁵ J. Konigsberg,¹⁶ A.V. Kotwal,¹⁴ M. Kreps,²⁴ J. Kroll,⁴³ D. Krop,¹¹ N. Krumnack^{l,5} M. Kruse,¹⁴ V. Krutelyov^{d,51} T. Kuhr,²⁴ M. Kurata,⁵³ S. Kwang,¹¹ A.T. Laasanen,⁴⁶ S. Lami,⁴⁴ S. Lammel,¹⁵ M. Lancaster,²⁸ R.L. Lander,⁷ K. Lannon^{u,37} A. Lath,⁵⁰ G. Latino^{cc,44} I. Lazzizzera,⁴¹ T. LeCompte,² E. Lee,⁵¹ H.S. Lee,¹¹ J.S. Lee,²⁵ S.W. Lee^{w,51} S. Leo^{bb,44} S. Leone,⁴⁴ J.D. Lewis,¹⁵ C.-J. Lin,²⁶ J. Linacre,⁴⁰ M. Lindgren,¹⁵ E. Lipeles,⁴³ A. Lister,¹⁸ D.O. Litvintsev,¹⁵ C. Liu,⁴⁵ Q. Liu,⁴⁶ T. Liu,¹⁵ S. Lockwitz,⁵⁹ N.S. Lockyer,⁴³ A. Loginov,⁵⁹ D. Lucchesi^{aa,41} J. Lueck,²⁴ P. Lujan,²⁶ P. Lukens,¹⁵ G. Lungu,⁴⁸ J. Lys,²⁶ R. Lysak,¹² R. Madrak,¹⁵ K. Maeshima,¹⁵ K. Makhoul,³⁰ P. Maksimovic,²³ S. Malik,⁴⁸ G. Manca^{b,27} A. Manousakis-Katsikakis,³ F. Margaroli,⁴⁶ C. Marino,²⁴ M. Martínez,⁴ R. Martínez-Ballarín,²⁹ P. Mastrandrea,⁴⁹ M. Mathis,²³ M.E. Mattson,⁵⁷ P. Mazzanti,⁶ K.S. McFarland,⁴⁷ P. McIntyre,⁵¹ R. McNulty^{i,27} A. Mehta,²⁷ P. Mehtala,²¹ A. Menzione,⁴⁴ C. Mesropian,⁴⁸ T. Miao,¹⁵ D. Mietlicki,³² A. Mitra,¹ H. Miyake,⁵³ S. Moed,²⁰ N. Moggi,⁶ M.N. Mondragon^{k,15} C.S. Moon,²⁵ R. Moore,¹⁵ M.J. Morello,¹⁵ J. Morlock,²⁴ P. Movilla Fernandez,¹⁵ J. Mülmenstädt,²⁶ A. Mukherjee,¹⁵ Th. Muller,²⁴ P. Murat,¹⁵ M. Mussini^{z,6} J. Nachtman^{m,15} Y. Nagai,⁵³ J. Naganoma,⁵⁶ I. Nakano,³⁸ A. Napier,⁵⁴ J. Nett,⁵⁸ C. Neu,⁵⁵ M.S. Neubauer,²²

J. Nielsen^{e,26} L. Nodulman,² O. Norniella,²² E. Nurse,²⁸ L. Oakes,⁴⁰ S.H. Oh,¹⁴ Y.D. Oh,²⁵ I. Oksuzian,⁵⁵ T. Okusawa,³⁹ R. Orava,²¹ L. Ortolan,⁴ S. Pagan Griso^{aa,41} C. Pagliarone,⁵² E. Palencia^{f,9} V. Papadimitriou,¹⁵ A.A. Paramonov,² J. Patrick,¹⁵ G. Pauletta^{ff,52} M. Paulini,¹⁰ C. Paus,³⁰ D.E. Pellett,⁷ A. Penzo,⁵² T.J. Phillips,¹⁴ G. Piacentino,⁴⁴ E. Pianori,⁴³ J. Pilot,³⁷ K. Pitts,²² C. Plager,⁸ L. Pondrom,⁵⁸ K. Potamianos,⁴⁶ O. Poukhov^{*,13} F. Prokoshin^{x,13} A. Pronko,¹⁵ F. Ptohos^{h,17} E. Pueschel,¹⁰ G. Punzi^{bb,44} J. Pursley,⁵⁸ A. Rahaman,⁴⁵ V. Ramakrishnan,⁵⁸ N. Ranjan,⁴⁶ I. Redondo,²⁹ P. Renton,⁴⁰ M. Rescigno,⁴⁹ F. Rimondi^{z,6} L. Ristori^{45,15} A. Robson,¹⁹ T. Rodrigo,⁹ T. Rodriguez,⁴³ E. Rogers,²² S. Rolli,⁵⁴ R. Roser,¹⁵ M. Rossi,⁵² F. Rubbo,¹⁵ F. Ruffini^{cc,44} A. Ruiz,⁹ J. Russ,¹⁰ V. Rusu,¹⁵ A. Safonov,⁵¹ W.K. Sakumoto,⁴⁷ L. Santi^{ff,52} L. Sartori,⁴⁴ K. Sato,⁵³ V. Saveliev^{t,42} A. Savoy-Navarro,⁴² P. Schlabach,¹⁵ A. Schmidt,²⁴ E.E. Schmidt,¹⁵ M.P. Schmidt^{*,59} M. Schmitt,³⁶ T. Schwarz,⁷ L. Scodellaro,⁹ A. Scribano^{cc,44} F. Scuri,⁴⁴ A. Sedov,⁴⁶ S. Seidel,³⁵ Y. Seiya,³⁹ A. Semenov,¹³ F. Sforza^{bb,44} A. Sfyrla,²² S.Z. Shalhout,⁷ M.D. Shapiro,²⁶ T. Shears,²⁷ P.F. Shepard,⁴⁵ M. Shimojima^{s,53} S. Shiraishi,¹¹ M. Shochet,¹¹ I. Shreyber,³⁴ A. Simonenko,¹³ P. Sinervo,³¹ A. Sissakian^{*,13} K. Sliwa,⁵⁴ J.R. Smith,⁷ F.D. Snider,¹⁵ A. Soha,¹⁵ S. Somalwar,⁵⁰ V. Sorin,⁴ P. Squillacioti,¹⁵ M. Stanitzki,⁵⁹ R. St. Denis,¹⁹ B. Stelzer,³¹ O. Stelzer-Chilton,³¹ D. Stentz,³⁶ J. Strologas,³⁵ G.L. Strycker,³² Y. Sudo,⁵³ A. Sukhanov,¹⁶ I. Suslov,¹³ K. Takemasa,⁵³ Y. Takeuchi,⁵³ J. Tang,¹¹ M. Tecchio,³² P.K. Teng,¹ J. Thom^{g,15} J. Thome,¹⁰ G.A. Thompson,²² E. Thomson,⁴³ P. Ttito-Guzmán,²⁹ S. Tkaczyk,¹⁵ D. Toback,⁵¹ S. Tokar,¹² K. Tollefson,³³ T. Tomura,⁵³ D. Tonelli,¹⁵ S. Torre,¹⁷ D. Torretta,¹⁵ P. Totaro^{ff,52} M. Trovato^{dd,44} Y. Tu,⁴³ N. Turini^{cc,44} F. Ukegawa,⁵³ S. Uozumi,²⁵ A. Varganov,³² E. Vataga^{dd,44} F. Vázquez^{k,16} G. Velev,¹⁵ C. Vellidis,³ M. Vidal,²⁹ I. Vila,⁹ R. Vilar,⁹ M. Vogel,³⁵ G. Volpi^{bb,44} P. Wagner,⁴³ R.L. Wagner,¹⁵ T. Wakisaka,³⁹ R. Wallny,⁸ S.M. Wang,¹ A. Warburton,³¹ D. Waters,²⁸ M. Weinberger,⁵¹ W.C. Wester III,¹⁵ B. Whitehouse,⁵⁴ D. Whiteson^{c,43} A.B. Wicklund,² E. Wicklund,¹⁵ S. Wilbur,¹¹ F. Wick,²⁴ H.H. Williams,⁴³ J.S. Wilson,³⁷ P. Wilson,¹⁵ B.L. Winer,³⁷ P. Wittich^{g,15} S. Wolbers,¹⁵ H. Wolfe,³⁷ T. Wright,³² X. Wu,¹⁸ Z. Wu,⁵ K. Yamamoto,³⁹ J. Yamaoka,¹⁴ T. Yang,¹⁵ U.K. Yang^{p,11} Y.C. Yang,²⁵ W.-M. Yao,²⁶ G.P. Yeh,¹⁵ K. Yi^{m,15} J. Yoh,¹⁵ K. Yorita,⁵⁶ T. Yoshida^{j,39} G.B. Yu,¹⁴ I. Yu,²⁵ S.S. Yu,¹⁵ J.C. Yun,¹⁵ A. Zanetti,⁵² Y. Zeng,¹⁴ and S. Zucchelli^{z6}

(CDF Collaboration[†])

¹*Institute of Physics, Academia Sinica, Taipei, Taiwan 11529, Republic of China*

²*Argonne National Laboratory, Argonne, Illinois 60439, USA*

³*University of Athens, 157 71 Athens, Greece*

⁴*Institut de Fisica d'Altes Energies, Universitat Autònoma de Barcelona, E-08193, Bellaterra (Barcelona), Spain*

⁵*Baylor University, Waco, Texas 76798, USA*

⁶*Istituto Nazionale di Fisica Nucleare Bologna, ^zUniversity of Bologna, I-40127 Bologna, Italy*

⁷*University of California, Davis, Davis, California 95616, USA*

⁸*University of California, Los Angeles, Los Angeles, California 90024, USA*

⁹*Instituto de Fisica de Cantabria, CSIC-University of Cantabria, 39005 Santander, Spain*

¹⁰*Carnegie Mellon University, Pittsburgh, Pennsylvania 15213, USA*

¹¹*Enrico Fermi Institute, University of Chicago, Chicago, Illinois 60637, USA*

¹²*Comenius University, 842 48 Bratislava, Slovakia; Institute of Experimental Physics, 040 01 Kosice, Slovakia*

¹³*Joint Institute for Nuclear Research, RU-141980 Dubna, Russia*

¹⁴*Duke University, Durham, North Carolina 27708, USA*

¹⁵*Fermi National Accelerator Laboratory, Batavia, Illinois 60510, USA*

¹⁶*University of Florida, Gainesville, Florida 32611, USA*

¹⁷*Laboratori Nazionali di Frascati, Istituto Nazionale di Fisica Nucleare, I-00044 Frascati, Italy*

¹⁸*University of Geneva, CH-1211 Geneva 4, Switzerland*

¹⁹*Glasgow University, Glasgow G12 8QQ, United Kingdom*

²⁰*Harvard University, Cambridge, Massachusetts 02138, USA*

²¹*Division of High Energy Physics, Department of Physics,*

University of Helsinki and Helsinki Institute of Physics, FIN-00014, Helsinki, Finland

²²*University of Illinois, Urbana, Illinois 61801, USA*

²³*The Johns Hopkins University, Baltimore, Maryland 21218, USA*

²⁴*Institut für Experimentelle Kernphysik, Karlsruhe Institute of Technology, D-76131 Karlsruhe, Germany*

²⁵*Center for High Energy Physics: Kyungpook National University,*

Daegu 702-701, Korea; Seoul National University, Seoul 151-742,

Korea; Sungkyunkwan University, Suwon 440-746,

Korea; Korea Institute of Science and Technology Information,

Daejeon 305-806, Korea; Chonnam National University, Gwangju 500-757,

Korea; Chonbuk National University, Jeonju 561-756, Korea

²⁶*Ernest Orlando Lawrence Berkeley National Laboratory, Berkeley, California 94720, USA*

- ²⁷University of Liverpool, Liverpool L69 7ZE, United Kingdom
²⁸University College London, London WC1E 6BT, United Kingdom
²⁹Centro de Investigaciones Energeticas Medioambientales y Tecnologicas, E-28040 Madrid, Spain
³⁰Massachusetts Institute of Technology, Cambridge, Massachusetts 02139, USA
³¹Institute of Particle Physics: McGill University, Montréal, Québec, Canada H3A 2T8; Simon Fraser University, Burnaby, British Columbia, Canada V5A 1S6; University of Toronto, Toronto, Ontario, Canada M5S 1A7; and TRIUMF, Vancouver, British Columbia, Canada V6T 2A3
³²University of Michigan, Ann Arbor, Michigan 48109, USA
³³Michigan State University, East Lansing, Michigan 48824, USA
³⁴Institution for Theoretical and Experimental Physics, ITEP, Moscow 117259, Russia
³⁵University of New Mexico, Albuquerque, New Mexico 87131, USA
³⁶Northwestern University, Evanston, Illinois 60208, USA
³⁷The Ohio State University, Columbus, Ohio 43210, USA
³⁸Okayama University, Okayama 700-8530, Japan
³⁹Osaka City University, Osaka 588, Japan
⁴⁰University of Oxford, Oxford OX1 3RH, United Kingdom
⁴¹Istituto Nazionale di Fisica Nucleare, Sezione di Padova-Trento, ^{aa}University of Padova, I-35131 Padova, Italy
⁴²LPNHE, Universite Pierre et Marie Curie/IN2P3-CNRS, UMR7585, Paris, F-75252 France
⁴³University of Pennsylvania, Philadelphia, Pennsylvania 19104, USA
⁴⁴Istituto Nazionale di Fisica Nucleare Pisa, ^{bb}University of Pisa, ^{cc}University of Siena and ^{dd}Scuola Normale Superiore, I-56127 Pisa, Italy
⁴⁵University of Pittsburgh, Pittsburgh, Pennsylvania 15260, USA
⁴⁶Purdue University, West Lafayette, Indiana 47907, USA
⁴⁷University of Rochester, Rochester, New York 14627, USA
⁴⁸The Rockefeller University, New York, New York 10065, USA
⁴⁹Istituto Nazionale di Fisica Nucleare, Sezione di Roma 1, ^{ee}Sapienza Università di Roma, I-00185 Roma, Italy
⁵⁰Rutgers University, Piscataway, New Jersey 08855, USA
⁵¹Texas A&M University, College Station, Texas 77843, USA
⁵²Istituto Nazionale di Fisica Nucleare Trieste/Udine, I-34100 Trieste, ^{ff}University of Trieste/Udine, I-33100 Udine, Italy
⁵³University of Tsukuba, Tsukuba, Ibaraki 305, Japan
⁵⁴Tufts University, Medford, Massachusetts 02155, USA
⁵⁵University of Virginia, Charlottesville, VA 22906, USA
⁵⁶Waseda University, Tokyo 169, Japan
⁵⁷Wayne State University, Detroit, Michigan 48201, USA
⁵⁸University of Wisconsin, Madison, Wisconsin 53706, USA
⁵⁹Yale University, New Haven, Connecticut 06520, USA

We present a measurement of the B_s^0 lifetime in fully and partially reconstructed $B_s^0 \rightarrow D_s^-(\phi\pi^-)X$ decays in 1.3 fb^{-1} collected in $p\bar{p}$ collisions at $\sqrt{s} = 1.96 \text{ TeV}$ by the CDF II detector at the Fermilab Tevatron. We measure $\tau(B_s^0) = 1.518 \pm 0.041 \text{ (stat.)} \pm 0.027 \text{ (syst.) ps}$. The ratio of this result and the world average B^0 lifetime yields $\tau(B_s^0)/\tau(B^0) = 0.99 \pm 0.03$, which is in agreement with recent theoretical predictions.

PACS numbers: 14.40.Nd, 13.25.Hw

In the spectator model of heavy hadron decay, the life-

*Deceased

†With visitors from ^aUniversity of Massachusetts Amherst, Amherst, Massachusetts 01003, ^bIstituto Nazionale di Fisica Nucleare, Sezione di Cagliari, 09042 Monserrato (Cagliari), Italy, ^cUniversity of California Irvine, Irvine, CA 92697, ^dUniversity of California Santa Barbara, Santa Barbara, CA 93106 ^eUniversity of California Santa Cruz, Santa Cruz, CA 95064, ^fCERN, CH-1211 Geneva, Switzerland, ^gCornell University, Ithaca, NY 14853, ^hUniversity of Cyprus, Nicosia CY-1678, Cyprus, ⁱUniversity College Dublin, Dublin 4, Ireland, ^jUniversity of Fukui, Fukui City, Fukui Prefecture, Japan 910-0017, ^kUniversidad Iberoamericana, Mexico D.F., Mexico, ^lIowa State University, Ames, IA 50011, ^mUniversity of Iowa, Iowa City, IA 52242, ⁿKinki University,

Higashi-Osaka City, Japan 577-8502, ^oKansas State University, Manhattan, KS 66506, ^pUniversity of Manchester, Manchester M13 9PL, England, ^qQueen Mary, University of London, London, E1 4NS, England, ^rMuons, Inc., Batavia, IL 60510, ^sNagasaki Institute of Applied Science, Nagasaki, Japan, ^tNational Research Nuclear University, Moscow, Russia, ^uUniversity of Notre Dame, Notre Dame, IN 46556, ^vUniversidad de Oviedo, E-33007 Oviedo, Spain, ^wTexas Tech University, Lubbock, TX 79609, ^xUniversidad Tecnica Federico Santa Maria, 110v Valparaiso, Chile, ^yYarmouk University, Irbid 211-63, Jordan, ^{gg}On leave from J. Stefan Institute, Ljubljana, Slovenia,

times of all b -hadrons are equal, independent of the flavor of the lighter quarks bound to the b quark. Using the heavy-quark expansion [1, 2] in the calculation of the width, spectator quark interactions enter in higher order $(\Lambda_{QCD}/m_b)^3$ terms where m_b is the mass of the b quark and Λ_{QCD} is the energy scale of the QCD interactions within the hadron. This leads to the lifetime hierarchy $\tau(B_s^0) \cong \tau(B^0) < \tau(B^+)$. Theoretical results predict $\tau(B^+)/\tau(B^0) = 1.06 \pm 0.02$ and $\tau(B_s^0)/\tau(B^0) = 1.00 \pm 0.01$ [3, 4]. The world averages for the corresponding experimental numbers are 1.071 ± 0.009 and 0.965 ± 0.017 , respectively [5]. The precision of our knowledge of the B_s^0 lifetime is much less than for the B^0 and B^+ lifetimes, and therefore, a more precise measurement would be useful, both in general and for comparison with theoretical calculations. Such a measurement is especially warranted since the agreement on the lifetime ratio between theory and experiment is only fair.

In this Letter, we present a measurement of the B_s^0 lifetime in flavor-specific decay modes. The data come from $p\bar{p}$ collisions at $\sqrt{s} = 1.96$ TeV at the Fermilab Tevatron. This analysis is based on an integrated luminosity of 1.3 fb^{-1} collected by the CDF II detector between February 2002 and November 2006. This sample yields more than 1100 fully-reconstructed $B_s^0 \rightarrow D_s^- \pi^+$ candidates with $D_s^- \rightarrow \phi \pi^-$ and $\phi \rightarrow K^+ K^-$ after online and offline selection [6]. In addition, the sample reconstructed as $B_s^0 \rightarrow D_s^- \pi^+$ includes partially-reconstructed (PR) B_s^0 candidates that are used in this lifetime measurement and more than double the number of B_s^0 candidates available for analysis. One such PR decay is $B_s^0 \rightarrow D_s^- \rho^+$ with $\rho^+ \rightarrow \pi^+ \pi^0$ where the π^0 is not reconstructed. The inclusion of PR decays introduces an uncertainty in the momentum measurement of a given candidate. However, a correction to the proper decay time has been estimated, and the total uncertainty on the lifetime measurement is improved by the use of the PR final states.

The CDF II detector is described in detail in Ref. [7]. The detector elements relevant for this analysis are the silicon vertex detectors [8–10] and the central drift chamber (COT) [11]. The silicon detectors consist of 7 or 8 layers of microstrip silicon sensors covering the pseudorapidity [12] range $|\eta| < 2.0$. The COT is an open cell drift chamber covering $|\eta| < 1.0$. Both the COT and silicon vertex detectors are immersed in a uniform 1.4 T axial magnetic field with the field axis parallel to the proton beam.

A data sample enriched in hadronic B decays is selected with a three-level trigger system that searches for tracks displaced from the primary vertex [13]. At level 1, patterns of hits in the COT are identified as tracks by the extremely fast tracker (XFT) [14]. At level 2, the silicon vertex trigger [15] associates a set of silicon hits with the XFT tracks and improves track measurement precision. The trigger requires each event to contain a pair of charged particle tracks, each having transverse momen-

tum $p_T \geq 2 \text{ GeV}/c$ and transverse impact parameter d_0 in the range $d_0 \in [120 \text{ } \mu\text{m}, 1 \text{ mm}]$, where d_0 is defined as the distance of closest approach between the particle trajectory and the beamline, measured in the transverse plane. The opening angle between the tracks' trajectories ($\Delta\phi$ in the plane transverse to the beam) must be between 2° and 90° , and their intersection must be at least $200 \text{ } \mu\text{m}$ from the interaction point, as measured in the plane transverse to the beam direction. At level 3 track reconstruction is performed entirely in software, with the full precision of the tracking system available, and the level 1 and 2 requirements are confirmed. These trigger requirements preferentially select events containing long-lived particles and sculpt the proper time distribution of the particles that are accepted for analysis. As the background rate of this trigger requires prescaling at higher instantaneous luminosities, CDF also employs two more restrictive triggers that require the tracks in the trigger pair to have opposite charges, individual $p_T \geq 2(2.5) \text{ GeV}/c$, and the scalar sum $p_T \geq 5.5(6.5) \text{ GeV}/c$.

We reconstruct $B_s^0 \rightarrow D_s^- \pi^+$ candidates (where B_s^0 and D_s^- imply B_s^0 candidates and D_s^- candidates) by first identifying $D_s^- \rightarrow \phi(K^- K^+) \pi^-$ from tracks with $p_T > 350 \text{ MeV}/c$ using the invariant mass requirements $|m(K^- K^+) - 1020.5| < 7.5 \text{ MeV}/c^2$ and $|m(K^- K^+ \pi^-) - 1968.3| < 20 \text{ MeV}/c^2$. The D_s^- daughter tracks must satisfy a three-dimensional vertex fit. We then combine each D_s^- with a positively charged track with $p_T > 1.0 \text{ GeV}/c$ to form a $B_s^0 \rightarrow D_s^- \pi^+$ candidate and require the pair to satisfy an additional three-dimensional vertex fit. We do not constrain the mass of the ϕ or D_s^- in this fit. The decay length of the B_s^0 is measured with respect to the event's primary vertex and must satisfy requirements on the following quantities: the decay length of the B_s^0 projected along the transverse momentum, $L_{xy}(B_s^0) > 450 \text{ } \mu\text{m}$, and its significance, $L_{xy}(B_s^0)/\sigma_{L_{xy}}(B_s^0) > 5$; the transverse distance between the B_s^0 and D_s^- decay points is greater than 0; the transverse impact parameter of the B_s^0 , $|d_0(B_s^0)| < 60 \text{ } \mu\text{m}$; and the significance of the longitudinal impact parameter, $|z_0(B_s^0)/\sigma_{z_0}(B_s^0)| < 3$. Both fits for the B_s^0 and D_s^- vertices must have reasonable goodness-of-fit values when considering only the track parameters measured in the transverse plane.

To further separate B_s^0 mesons from backgrounds with similar topologies, we require the transverse momentum of the B_s^0 , $p_T(B_s^0) > 5.5 \text{ GeV}/c$, and the angular separation between the D_s^- and the π from the B_s^0 , $\Delta R(D_s^-, \pi_B) = \sqrt{(\Delta\eta)^2 + (\Delta\phi)^2} < 1.5$. We require the isolation of the B_s^0 to be greater than 0.5, defined as $p_T(B_s^0)$ divided by the scalar sum of the transverse momenta of all the tracks in a cone of $\Delta R < 1$ around the B_s^0 . We tighten the requirement on the mass of the D_s^- ($|m - 1968.3| < 12 \text{ MeV}/c^2$) and veto D_s^- candidates consistent with $D^{*-} \rightarrow \bar{D}^0 \pi^-$ where the \bar{D}^0 decays to $K^+ \pi^- \pi^0$. The D^* veto is accomplished

by taking the D_s^- daughter tracks ($K^-K^+\pi^-$), assigning the pion mass to the negative kaon, and requiring $\Delta m = m(K^+\pi^-\pi^-) - m(K^+\pi^-) > 180 \text{ MeV}/c^2$. We also require that the decay contain two reconstructed tracks satisfying the level 2 trigger requirements.

The simulated data samples used in this analysis consist of single b -hadrons generated by BGENERATOR [16, 17] with p_T spectra consistent with NLO QCD and decayed with EVTGEN [18]. Full detector and trigger simulations are performed. The simulated B candidates are reconstructed with the same procedure and the same selection as the data candidates. We reweight the simulated sample to match the data distributions for $p_T(B)$ and trigger mixture.

The lifetime of the B_s^0 meson is determined from two sequential fits. The first is a fit to the invariant mass distribution of candidates reconstructed as $D_s^- \pi^+$ used to determine the fractions of the total number of events found in the various decay modes. These fractions are then used as fixed inputs in the second fit to the proper decay time distributions of the B_s^0 . The uncertainties on the fractions returned by the mass fit are treated as sources of systematic uncertainty.

The mass fit is an unbinned maximum likelihood fit to the invariant mass of the candidate reconstructed as $D_s^- \pi^+$ with $m_B^{rec} \in [4.85, 6.45] \text{ GeV}/c^2$. The mass fit components can be characterized as coming from one of three possible sources: single b -hadrons, real- D_s^- +track background, and fake- D_s^- +track background. The mass probability distribution functions (PDFs) for single b -hadrons were obtained from simulation, with an additional small shift and resolution smearing to bring the simulated B_s^0 -peak central value and width into agreement with data. The single- b modes were separated in the fit as follows: $B_s^0 \rightarrow D_s^- \pi^+(n\gamma)$, $B_s^0 \rightarrow D_s^\pm K^\mp$, $B_s^0 \rightarrow D_s^- \rho^+$, $B_s^0 \rightarrow D_s^{*-} \pi^+$, $B_s^0 \rightarrow D_s^{(*)} X$, $B^0/B^- \rightarrow D^- X$, $B^0 \rightarrow D_s^{(*)} \pi^+ + D_s^{(*)} K^+$, and $\Lambda_b \rightarrow \Lambda_c X$. The $D_s^\pm K^\mp/D_s^- \pi^+$ ratio was constrained to the results of Ref. [19].

Real- D_s^- +track backgrounds consist of a real D_s^- , produced promptly or from a b -hadron decay, plus an additional track produced in the event. The mass PDF for these events is obtained from an auxiliary fit to the wrong-sign sample, which consists of data events reconstructed as $D_s^- \pi^-$ and sideband subtracted in the D_s^- mass. The mass PDF for the fake- D_s^- +track background is obtained from an auxiliary fit to the D_s^- sidebands. The results of the mass fit are shown in Fig. 1 with various modes combined for plotting only. The real- D_s^- +track background and fake- D_s^- +track background components are drawn together as the ‘‘combinatorial background’’.

For the lifetime fit, the variable of interest is the proper decay time, defined as $ct \equiv (L_{xy}(B_s^0) \cdot m_B^{rec})/p_T(B_s^0)$. The reconstructed mass m_B^{rec} is used instead of the world av-

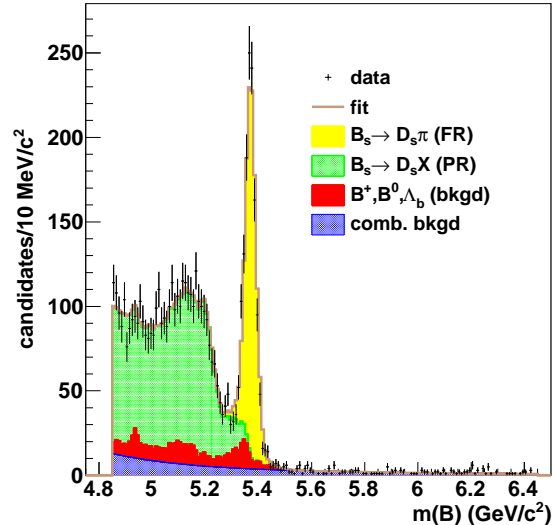


FIG. 1: Mass distribution for candidates reconstructed as $B_s^0 \rightarrow D_s^- \pi^+$ with fit projections overlaid.

erage B_s^0 mass. A salient feature of this analysis is the treatment of partially-reconstructed B_s^0 mesons as signal events that contribute to the lifetime measurement. Since in the partially-reconstructed cases $L_{xy}(B_s^0)$, m_B^{rec} , and $p_T(B_s^0)$ are extracted from candidates that are missing particles after reconstruction or have the wrong mass assignment for a daughter particle, a multiplicative correction factor K to the decay time is needed. K is defined as $K = [p_T(B_s^0) \cdot m_B^{true}] / [p_T^{true}(B_s^0) \cdot m_B^{rec} \cdot \cos \theta_{PR}]$ where θ_{PR} is the angle in the $x-y$ plane between the true momentum of the B_s^0 and the momentum of the partially-reconstructed B_s^0 . Because the ratio $m_B^{rec}/p_T(B_s^0)$ is numerically very close to the ratio $m_B^{true}/p_T^{true}(B_s^0)$, this choice of ct definition forces the K factor distributions to be centered near $K = 1$ with widths of a few percent. The K factor distributions are determined with simulation.

The lifetime of the B_s^0 meson is determined from an unbinned likelihood fit to the B_s^0 candidates with invariant masses in the range $[5.00, 5.45] \text{ GeV}/c^2$. There are three main types of lifetime fit components that will be described in the following paragraphs: fully-reconstructed B_s^0 , partially-reconstructed B_s^0 , and backgrounds. The treatment of each component depends on its decay structure and whether it can provide information about the B_s^0 lifetime.

Fully-reconstructed (FR) modes where all of the B_s^0 daughter particles are included with the correct mass assignment in the construction of the B_s^0 candidate are the first type of lifetime fit component. The only FR mode in this analysis is the $D_s^- \pi^+$. The core functional form of the FR PDF is an exponential with decay constant

$c\tau(B_s^0)$ convoluted with a Gaussian resolution function with width σ :

$$P_{\text{FR}}(ct) = \left[\frac{1}{c\tau} e^{-\frac{ct'}{c\tau}} \otimes_{t'} \frac{1}{\sqrt{2\pi}\sigma} e^{-\frac{(ct-ct')^2}{2\sigma^2}} \right] \cdot \text{eff}(ct) \quad (1)$$

A multiplicative ‘‘efficiency curve’’ accounts for the trigger and analysis selection criteria:

$$\text{eff}(ct) = \sum_{i=1}^3 N_i \cdot (ct - \beta_i)^2 \cdot e^{-\frac{ct}{\tau_i}} \cdot \theta(\beta_i)$$

The shape parameters (σ , β_i , N_i and τ_i) of the PDF are determined in a fit to a simulated B_s^0 sample where the lifetime used for generation is known. All the parameters for the PDF are then fixed and only $\tau(B_s^0)$ is varied in the final fit to the data. As we depend on the simulation of the displaced-track trigger, we use a data sample of $J/\psi \rightarrow \mu^+\mu^-$ decays collected with a di-muon trigger to assess the accuracy of this assumption and assign a ‘‘trigger simulation’’ systematic uncertainty based on these studies. The partially-reconstructed, PHOTOS-modeled $D_s^- \pi(n\gamma)$ decays [20] are combined with the FR $D_s^- \pi$, as the momentum carried by the photon is small and their lifetime distribution is extremely close to the FR one. This simplification is considered as a possible source of systematic uncertainty.

Partially-reconstructed modes either neglect B_s^0 daughter particles in the construction of the B_s^0 candidate or assign them an incorrect mass. $B_s^0 \rightarrow D_s^- K^+$, $D_s^- \rho^+$, $D_s^{*-} \pi^+$, and other decay modes partially reconstructed under the $D_s^- \pi^+$ hypothesis can also contribute to the B_s^0 lifetime measurement. The PR PDF is similar to the FR PDF of Eq. (1) with an additional convolution with the K factor distribution for each mode. There are separate efficiency curve parameters for each mode, again determined from fits to simulated events.

The backgrounds in the lifetime fit can either come from decays of b -hadrons other than the B_s^0 (e.g., $B^0/B^- \rightarrow D^- X$, $B^0 \rightarrow D_s^- X$, and $\Lambda_b \rightarrow \Lambda_c X$), or they can come from real- D_s^- +track and fake- D_s^- +track combinations. The PDFs for the former modes are derived from fits to simulated B^0 , B^- and Λ_b samples, while the ones for the latter combinatorial backgrounds come from the two proxies available: the B_s^0 upper sideband taken from the m_B^{rec} interval [5.7, 6.4] GeV/ c^2 and the D_s^- sidebands. The D_s^- sidebands are taken from the m_B^{rec} interval [5.0, 5.45] GeV/ c^2 and the m_D^{rec} interval [1.924, 1.939] \cup [1.999, 2.014] GeV/ c^2 . Both proxies contain a mixture of fake D_s^- +track events and real D_s^- +track events, where a real D_s^- can be poorly reconstructed. All the background shape parameters are fixed in the final lifetime fit.

The analysis procedure was tested extensively on three control samples: $B^0 \rightarrow D^- \pi^+$ with $D^- \rightarrow K^+ \pi^- \pi^-$,

$B^0 \rightarrow D^{*-} \pi^+$ with $D^{*-} \rightarrow \bar{D}^0 \pi^-$ and $\bar{D}^0 \rightarrow K^+ \pi^-$, and $B^+ \rightarrow \bar{D}^0 \pi^+$ with $\bar{D}^0 \rightarrow K^+ \pi^-$ before performing the B_s^0 fits. Furthermore, the lifetime fit of the B_s^0 was performed using a *blind* approach, i.e. by determining the statistical and systematic uncertainties without knowledge of the fit result itself. Good agreement with the world average values [5] of the B^0 and B^+ lifetimes was found.

The lifetime of $\tau(B_s^0) = 1.518 \pm 0.041$ (stat.) ps is obtained from the full fit. The fit results are plotted in Fig. 2. The results of the fits performed separately in the FR mass region (1.456 ± 0.067 ps) and PR mass region (1.544 ± 0.051 ps) agree with each other at a level of 1.0 σ .

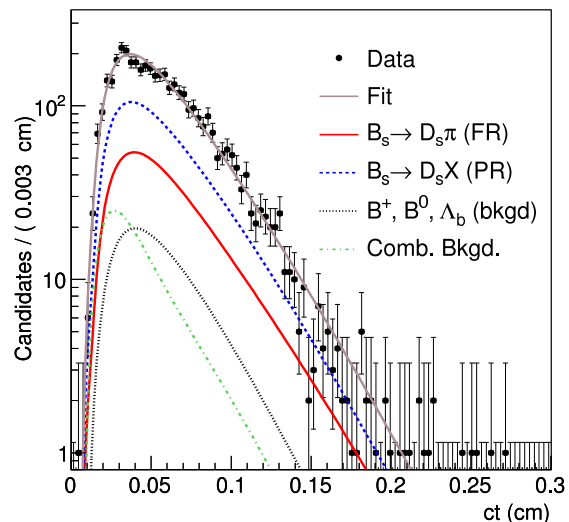


FIG. 2: Distribution of ct for candidates reconstructed as $B_s^0 \rightarrow D_s^- (\phi\pi^-)\pi^+$ with fit projection overlaid.

TABLE I: Summary of sources of systematic uncertainty for the $B_s^0 \rightarrow D_s^- (\phi\pi^-)X$ lifetime fit. The total uncertainty is calculated assuming the individual contributions are uncorrelated.

Description	Value (ps)
Background modeling and fractions	0.019
Fixed single- b background ct	0.003
Reweighting for p_T and trigger	0.012
Lifetime contribution of $D\pi$ radiative tail	0.002
Efficiency curve parameterization	0.002
Trigger simulation	0.014
Impact parameter correlation	0.003
Detector alignment	0.003
Total systematic uncertainty	0.027

We use a Monte Carlo technique to assess the systematic uncertainties. For each source of systematic uncertainty, we generate 1000 simulated experiments with the number of events in each experiment Poisson-distributed around the number of events in data. The simulated experiments are generated with a non-standard lifetime fit configuration (where the PDFs or numbers of events in the various modes are modified to account for the systematic effect) and fit with the default configuration. The mean biases returned from the fits to the simulated experiments ($\tau_{\text{ret}} - \tau_{\text{gen}}$) are used to set the size of the systematic uncertainties. We consider several sources of systematic uncertainty: combinatorial background fraction, modeling of backgrounds from single b -hadron decays, effect of reweighting the full simulations to match the data, modeling of the trigger bias as a function of ct , offline-online impact parameter correlation, accuracy of the trigger simulation in Monte Carlo, and detector alignment. Table I contains the final list of systematic uncertainties for this measurement. The largest contribution comes from the uncertainty on the total amount of combinatorial background and the amount of promptly produced real- D_s^- background.

The displaced-track trigger, in addition to modifying the accepted decay length distribution from a simple exponential to the form in Eq. (1), alters the expected mixture of mass eigenstates $B_{s,L}^0$ and $B_{s,H}^0$ in the flavor-specific $B_s^0 \rightarrow D_s^- \pi^+$ decay by preferentially selecting the longer lived $B_{s,H}^0$. The size of the imbalance can be calculated using the parameters of the efficiency curve and the world average of $1/\Gamma = 1.47$ ps [5]. Our result can be corrected back to a flavor-specific lifetime measurement with $\delta\tau(B_s^0) = -0.11(\Delta\Gamma/\Gamma)^2$ ps. Given the world average $\Delta\Gamma/\Gamma = 0.092_{-0.054}^{+0.051}$ [5], the correction would be smaller than our statistical and systematic uncertainties. Therefore, we do not correct the central value or assess an additional systematic uncertainty.

In summary we have measured the B_s^0 lifetime using both fully reconstructed $B_s^0 \rightarrow D_s^- (\phi\pi^-)\pi^+$ and partially reconstructed $B_s^0 \rightarrow D_s^- (\phi\pi^-)X$ decay modes, in a sample with 1.3 fb^{-1} of integrated luminosity. We measure $\tau(B_s^0) = 1.518 \pm 0.041$ (stat.) ± 0.027 (syst.) ps, which is consistent with theoretical expectations [3, 4].

We thank the Fermilab staff and the technical staffs of the participating institutions for their vital contributions. This work was supported by the U.S. Department of Energy and National Science Foundation; the Italian Istituto Nazionale di Fisica Nucleare; the Ministry of Education, Culture, Sports, Science and Technology of Japan; the Natural Sciences and Engineering Research Council of Canada; the National Science Council of the Republic of China; the Swiss National Science

Foundation; the A.P. Sloan Foundation; the Bundesministerium für Bildung und Forschung, Germany; the Korean World Class University Program, the National Research Foundation of Korea; the Science and Technology Facilities Council and the Royal Society, UK; the Institut National de Physique Nucleaire et Physique des Particules/CNRS; the Russian Foundation for Basic Research; the Ministerio de Ciencia e Innovación, and Programa Consolider-Ingenio 2010, Spain; the Slovak R&D Agency; the Academy of Finland; and the Australian Research Council (ARC).

-
- [1] G. Bellini, I. I. Y. Bigi, and P. J. Dornan, *Phys. Rep.* **289**, 1 (1997).
 - [2] I. I. Y. Bigi *et al.*, in *B Decays*, 2nd ed., edited by S. Stone (World Scientific, Singapore, 1994).
 - [3] F. Gabbiani, A. I. Onishchenko, and A. A. Petrov, *Phys. Rev. D* **70**, 094031 (2004).
 - [4] C. Tarantino, *Eur. Phys. J. C* **33** (2004) S895.
 - [5] K. Nakamura *et al.* (Particle Data Group), *J. Phys. G* **37**, 075021 (2010).
 - [6] Reference to the charge conjugate modes is implied throughout this Letter.
 - [7] D. Acosta *et al.* (CDF Collaboration), *Phys. Rev. D* **71**, 032001 (2005).
 - [8] A. Sill *et al.* (for the CDF Collaboration), *Nucl. Instrum. Methods A* **447**, 1 (2000).
 - [9] C. S. Hill (on behalf of the CDF Collaboration), *Nucl. Instrum. Methods, A* **530**, 1 (2004).
 - [10] A. Affolder *et al.*, *Nucl. Instrum. Methods, A* **453**, 84 (2000).
 - [11] T. Affolder *et al.*, *Nucl. Instrum. Methods A* **526**, 249 (2004).
 - [12] CDF II uses a right-handed coordinate system with the origin at the center of the detector, in which the z axis is along the proton direction, the y axis points up, θ and ϕ are the polar and azimuthal angles, and r is the radial distance in the xy plane. The pseudorapidity η is dened as $\log \tan(\theta/2)$.
 - [13] A. Abulencia *et al.* (CDF Collaboration), *Phys. Rev. D* **74**, 072006 (2006).
 - [14] E. J. Thomson *et al.*, *IEEE Trans. on Nucl. Sci.* **49**, 1063 (2002).
 - [15] W. Ashmanskas *et al.* (for the CDF Collaboration), *Nucl. Instrum. Methods A* **518**, 532 (2004).
 - [16] P. Nason, S. Dawson, and R. K. Ellis, *Nucl. Phys.* **B303**, 607 (1988).
 - [17] P. Nason, S. Dawson, and R. K. Ellis, *Nucl. Phys.* **B327**, 49 (1989).
 - [18] D. J. Lange, *Nucl. Instrum. Methods A* **462**, 152 (2001).
 - [19] T. Aaltonen *et al.* (CDF Collaboration), *Phys. Rev. Lett.* **103**, 191802 (2009).
 - [20] E. Barberio and Z. Was, *Comput. Phys. Commun.* **79**, 291 (1994).